We are IntechOpen, the world's leading publisher of Open Access books
Built by scientists, for scientists

6,900
Open access books available

186,000
International authors and editors

200M
Downloads

Our authors are among the

154
Countries delivered to

TOP 1%
most cited scientists

12.2%
Contributors from top 500 universities

Interested in publishing with us?
Contact book.department@intechopen.com

Numbers displayed above are based on latest data collected.
For more information visit www.intechopen.com

Tuning Fork Scanning Probe Microscopes – Applications for the Nano-Analysis of the Material Surface and Local Physico-Mechanical Properties

Vo Thanh Tung[1,3], S.A. Chizhik[2], Tran Xuan Hoai[3],
Nguyen Trong Tinh[3] and V.V. Chikunov[2]
[1]Hue University of Sciences
[2]A.V. Luikov Heat and Mass Transfer Institute of
National Academy of Sciences of Belarus
[3]Institute of Applied Physics and Scientific Instrument of
Vietnamese Academy of Science and Technology
[1,3]Vietnam
[2]Belarus

1. Introduction

The atomic force microscopes (AFMs) or scanning force microscopes (SFMs) are a very high resolution type of scanning probe microscope (SPM), with demonstrated resolutions of a fraction of a nanometer. The AFMs are one of the foremost tools for imaging, measuring and manipulating matters at the nanoscale level. AFMs operate by measuring the atomic interaction (attractive or repulsive) forces between a tip and a sample [1]. Today, most AFMs employ an optical lever sensor - an expensive system that can achieve pico-meter resolution. The optical lever (Fig.1 (a)) operates by reflecting a laser beam off the cantilever. The angular deflection of the cantilever causes a large twofold of the laser beam. The reflected laser beam strikes a position sensing photodetector consisting of two side-by-side photodiodes. The difference between the two photodiode signals indicates the position of the laser spot on the detector and thus the angular deflection of the cantilever. Because the cantilever-to-detector distance generally measures thousands of times the length of the cantilever, the optical lever greatly magnifies motions of the tip [2]. The advantages of optical lever are possibility to measure absolute force and commercial available but there are many disadvantages: external optical measuring system needed, very low stiffness, fragile and high cost of AFM.

Recently, the quartz tuning fork sensors (QTFs) are being developed and it is well established that quartz tuning forks can be used as sensors for acoustic [3] and force microscopy [4]. Quartz tuning forks were originally introduced into the field of scanning probe microscopy (SPM) by Gunther *et al.* [3], and later by Karrai and Grober [5]. Giessibl *et al.* [6] employed them for atomic resolution AFM imaging. Tuning forks were used as sensors at low temperatures and in high magnetic fields by Rychen *et al.* [7]. The forks have several advantages: high amplitude and phase sensitivities, high mechanical quality factor
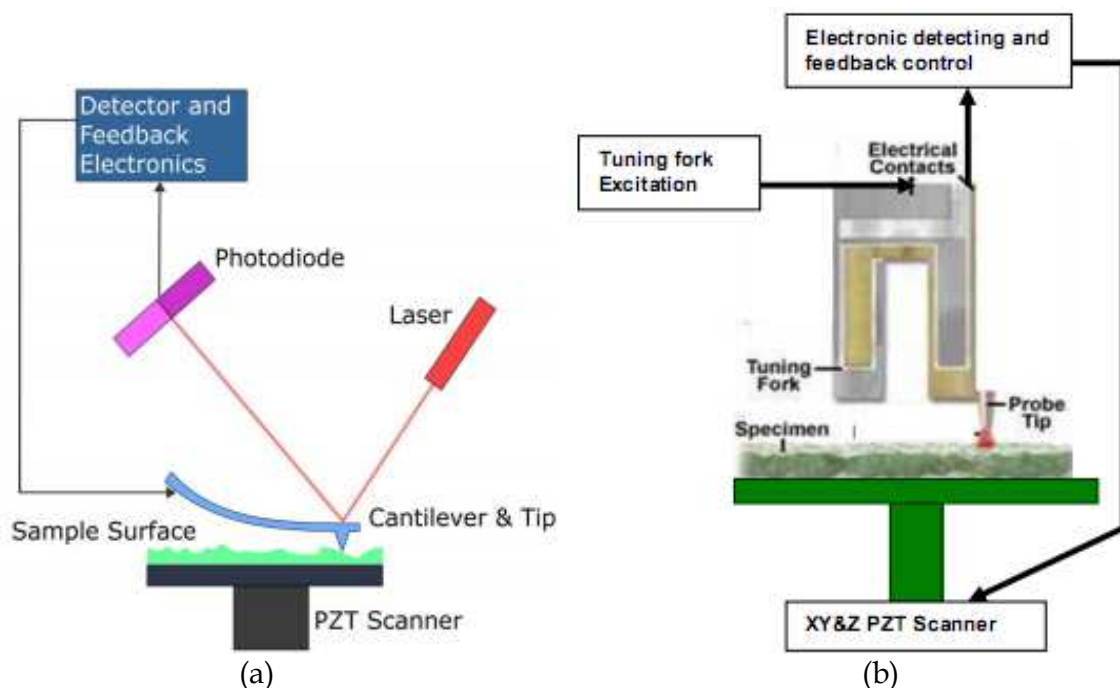
Fig. 1. (a) The traditional AFM (b) AFM with Tuning fork sensor

Q, large spring constant which allows the detection of pico-newton forces and the acquisition of true atomic resolution images. Their advantage is that the measurement of their oscillation amplitude uses the piezoelectric effect native to quartz crystal, yielding an electrical signal correlated to the applied forces (amplitude, phase and resonance frequency are correlated to the applied force) and making them small, robust and simple to operate compared to optical force measurement schemes. The feedback control can be constructed in a fully digital-electronic manner, so that the implementation of the feedback control is greatly simplified. The quartz tuning forks have been successfully demonstrated under various conditions [3, 5, 7-9].

K. Karrai and I. Tiemann [10] reported the results of the measurements with a tuning fork that was able to detect the friction force in the pN range. In their measurements, the tuning fork was excited by mechanical coupling with an external piezo oscillator, so that the Q-factor of the system could not be controlled. Furthermore K. Karrai and I. Tiemann reported difficulty in obtaining images with tuning fork sensors in air and liquid environments due to fluctuations of the resonant frequency.

Recently, electronic devices have been developed that allow the Q factor of an oscillating tuning fork in an AFM to be varied in a controlled manner [11]. It was possible to lower the Q factor of the probe, reducing the scanning time of the microscope accordingly. In these cases, not only did the images have a better signal-to-noise ratio, but they were also obtained at a faster scan speed. More details on the relation between the Q factor of the probe and the microscope sensitivity can be found in previous publications [12, 13, 14].

In this chapter, we demonstrate atomic force microscopes in the ambient conditions using the Q control for quartz tuning fork. We will describe the use of the tuning fork as a force sensor and use it in some applications of scanning probe microscopy (Fig.1 (b)). The advantages and disadvantages of a device with Q controlled will be discussed also.

2. Quartz tuning fork

A tuning fork is a two-pronged, metallic fork with the tine formed from a U-shaped bar of elastic material (usually steel). A tuning fork resonates at a specific constant pitch when set vibrating by e.g. striking it against a surface or with an object, and after waiting a moment to allow some high overtones to die out. The pitch generated by a particular tuning fork depends on the length of the two prongs, with two nodes near the bend of the U [15-17].

Figure 2 (a) shows a picture of the tuning fork appears as a metallic cylinder 8 mm in height, by 3 mm in diameter, holding a two-terminal electronic component. The packaging of the tuning fork can easily be opened by using tweezers to clamp the cylinder until the bottom of the cylinder breaks. A more reproducible way to open the packaging is to use a model-making saw to cut the metallic cylinder, keeping the bottom insulator as a holder to prevent the contact pins from breaking (Fig. 2 (b)).
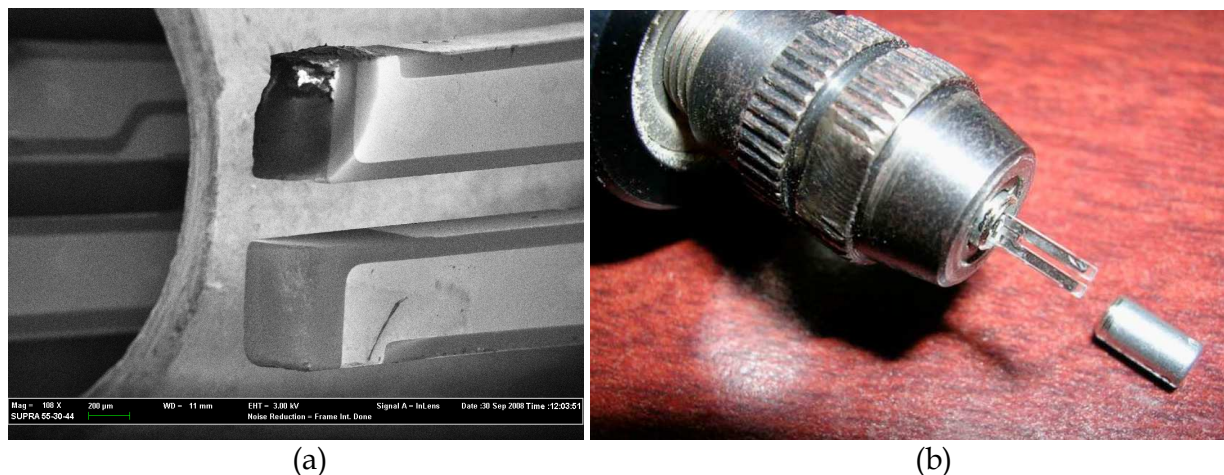

Fig. 2. (a) SEM image of tuning fork displaying the layout of the electrodes. (b) A tuning fork just removed from its packing, and the metallic enclosure that would otherwise keep it under vacuum.

Quartz tuning forks are primarily designed for frequency controls and time-based applications. Furthermore, applications of quartz tuning fork resonators seem to be an attractive alternative to the conventional mass measurement techniques since the tuning fork resonators combine the high Q-factor in the ambience of a quartz resonator and the flexural oscillation mode of a cantilever [18]. A number of tuning fork designs were developed that exploits the mechanical resonance such as flexure, extensional, torsion and shear modes. The sensitivity of these mode frequencies to external perturbations such as mass loading, force, pressure, and temperature quartz oscillators are suitable for sensor technologies [8, 19-21].

A tuning fork of a commercially available type fabricated for "quartz" clocks was used (type 74-530-04 of ELFA Company with a standard resonance frequency 32757Hz, and a theoretical quality factor Q=15000). The fork was modeled in a standard way as a series R-L-C circuit. The R-L-C model provides a convenient electrical analogue to the mechanical properties of the tuning fork. (Its mass m, stiffness or spring constant k, and damping due to internal and external dissipative forces are represented by L, C, and R respectively.) This model is usually further improved by the inclusion of a parallel shunt capacitance Co corresponding to the package capacitance. The admittance was measured as a function of

frequency using a signal synthesizer and lock-in amplifier. The theoretical spring constant is obtained from the formula $k = \frac{E}{4} W \left(\frac{T}{L} \right)^3$ [22] where $E = 7,87.10^{10} \, N/m^2$ is the Young modulus of quartz. The length (L), thickness (T) and width (W) of the tuning fork used are 6.01, 0.35 and 0.61 mm, respectively. Using these parameters, we obtain k ≈ 7kN/m, which agrees reasonably well with our experimental result.

3. Tips and probes

The tips attached to the prong of the tuning fork were silicon tips and tungsten tips. The tip was placed on the tuning fork using an optical microscope equipped with a micro-positioning stage. The mass of the silicon tip was so small that the reduction in the quality factor as well as the resonance-frequency shift of the fork was very small (both changes were less than 1%). For the tungsten tip, it was fabricated by electrochemical etching achieving a radius of about 30-70nm. When the tip was glued directly to a prong of a tuning fork, the quality factor decreased from 14000 to 7000-9000.

A method of connecting a tip (silicon tips or tungsten tips) to the tuning fork is gluing with two component epoxy. Epoxy glue was chosen because of its strong adhesive properties and the drying rate was not too fast. The added mass by the glue was able negligibly small. Figure 3a shows the result of this process with a tungsten tip across attached to one prong of the tuning fork. Figure 3b shows the result of a very sharp silicon tip only a few ten of micrometers attached to one prong of the tuning fork. Figure 4 represents the resonance curves of amplitude in ambience for a tuning fork before, and after it is mounted with a tip on one prong, as described earlier.
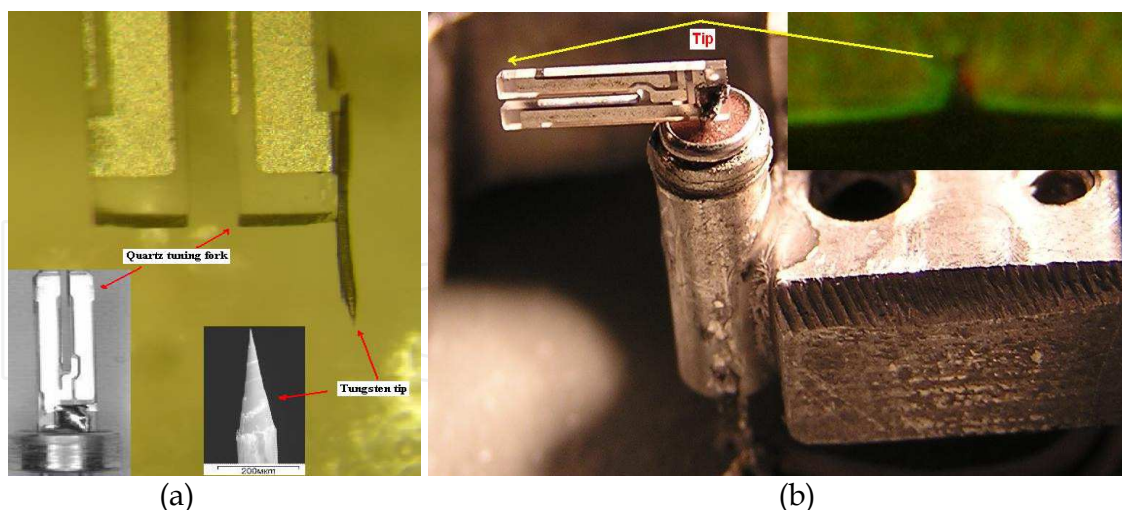

(a)   (b)

Fig. 3. Image of tungsten tip (a) and silicon tips (b) attached to tuning fork face surface

4. Principle operation of quartz tuning fork base on atomic force microscopy (Fork-AFM)

A scanning probe microscope, based on the above described quartz tuning fork, is shown in Fig. 5 (a). The mechanical part of the tuning fork that connecting to the atomic force

Tuning Fork Scanning Probe Microscopes – Applications for the
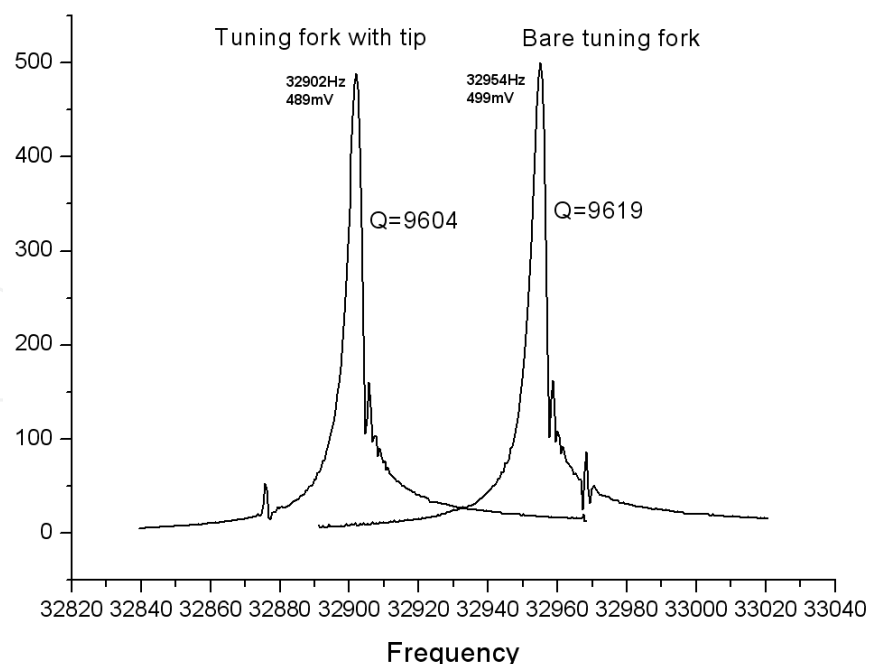Nano-Analysis of the Material Surface and Local Physico-Mechanical Properties

37

Fig. 4. Spectrum of bare tuning fork and tuning fork with commercial AFM cantilever tip

microscopy is shown in Fig. 5 (b). This mechanical part consists of two main units: a holder (1) and a base plate (2). The holder is designed as the unit housing most of the mechanical components of the shear force microscope. Two fine-pitch screws (4) are fixed to the holder in the standard arrangement for probe-sample coarse and fine approaching. The tuning fork sensor (5) as the heart of the system is attached to the holder with cyanoacrylate glue, and connected to the AFM through the cable (8). The holder with tuning fork is placed on the base plate (2) and secured using the outside metal box (6). The metal box could be moved in the sample state (7).

There are two basic methods of dynamic operation: intermittent contact mode and shear-force (or lateral mode) operation. Figure 5 (c) displays the basic principle of Fork-AFM in ambient conditions using a quartz tuning fork in these modes. As shown in Fig. 5 (c-lower part), the tip is mounted perpendicular to the tuning-fork prong so that the tip oscillates perpendicularly to the sample surface. This is the intermittent contact mode. In the lateral force sensor mode (Fig. 5 (c-upper part)), the tip is mounted parallel to the tuning fork prong and oscillates nearly parallel to the surface of a sample.

A constant sine wave voltage is applied to the one of the connectors of the tuning fork to drive the fork sensor. The other connector of the tuning fork is connected to a reference signal generator of a lock-in amplifier. An I-V converter is used to convert the net current to a voltage (Fig. 6). The current to voltage (I –V) gain of the circuit is calibrated from dc to 100 kHz. Under the resonant condition, the tuning fork arm has the biggest displacement that corresponds to the maximum or peak output voltage amplitude. The upper current-to-voltage converter will sense both the piezoelectric currents from the tuning fork oscillation and additional stray currents. The lower op-amp in Fig. 6 is not always necessary. However, it is present in order to cancel currents from stray capacitance (Co and other capacitance from wires). The lower op-amp (I- V) converter allows the cancellation of stray currents by adjusting the variable capacitor away from the resonance.
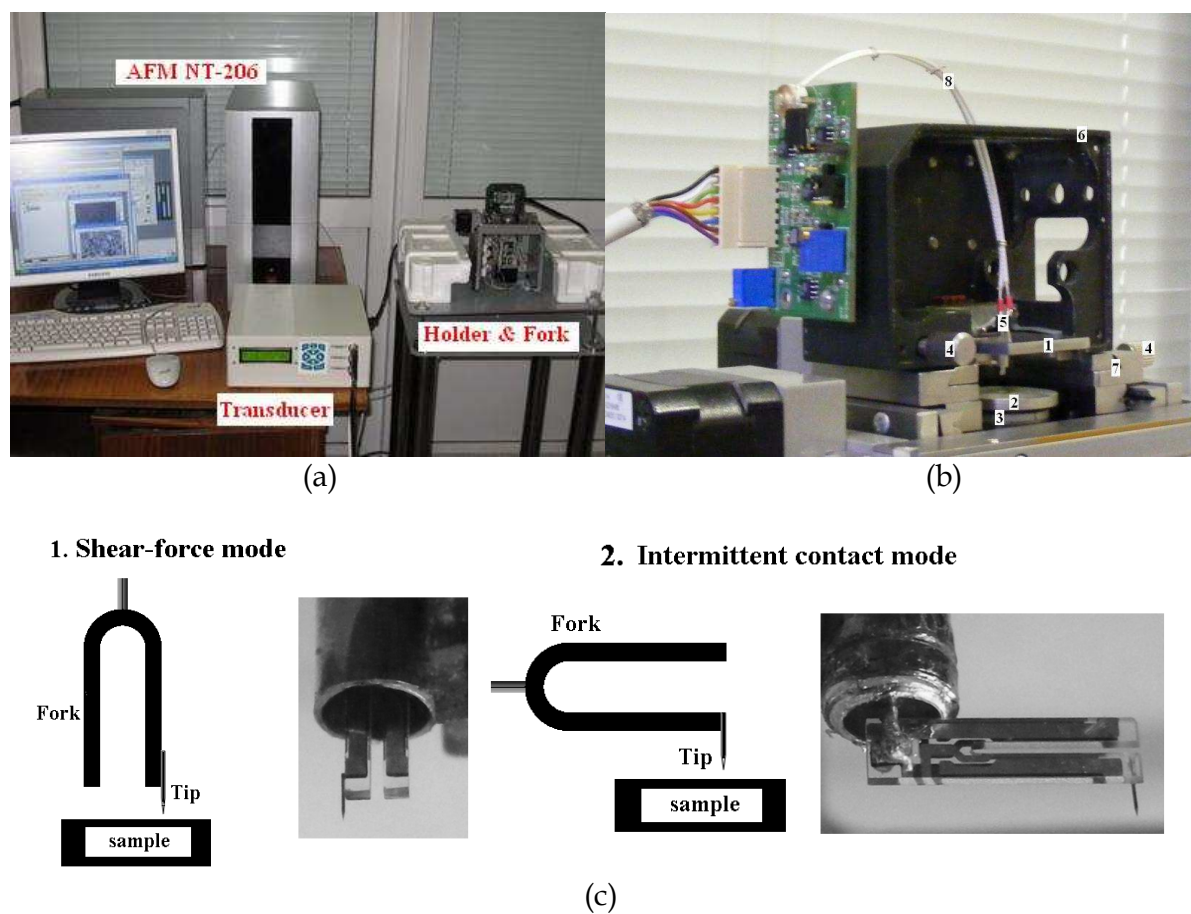
(a)   (b)

(c)

Fig. 5. (a) Photography of Atomic force microscopy using a quartz tuning fork (Fork-AFM) (b) Header of AFM using a quartz tuning fork (Fork-AFM) (1– holder, 2– base plate, 3– piezoscanner, 4– screws, 5– tuning fork sensor, 6– metal box, 7– sample state, 8– cable). (c) Principle of two operation modes: shear-force and intermittent contact mode.
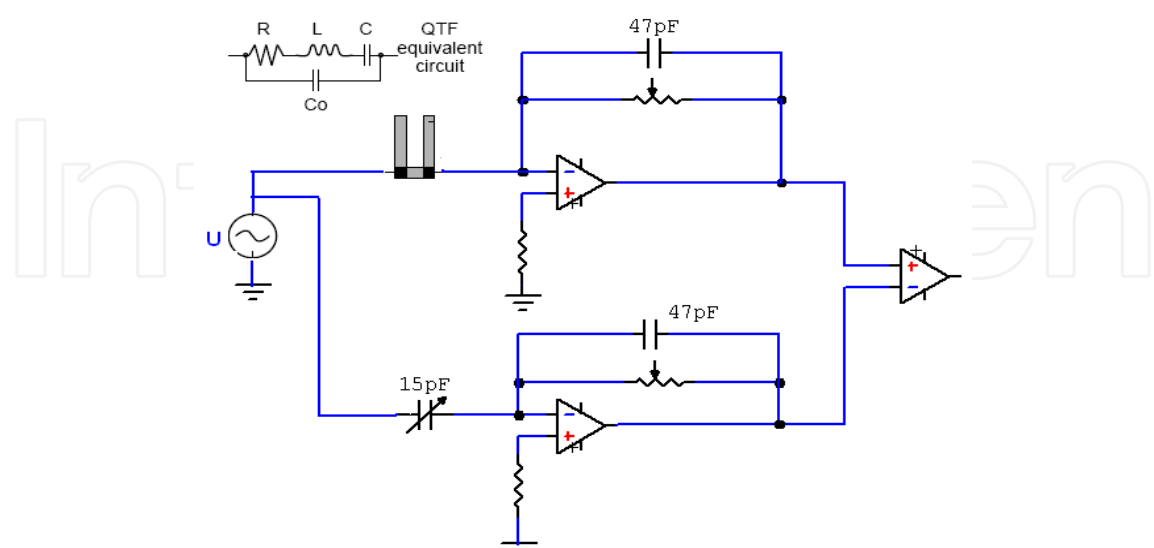

Fig. 6. Essential features of tuning fork sensing system and the equivalent circuit. Current through the tuning fork is converted to a voltage by an Op-Amp (OA). The lock-in reference signal is derived directly from the driving source and is not shown.

When the probe is approaching near the sample surface, the oscillation of the sensor is dampened due to probe-sample force interactions, resulting in a decrease in the output signal of the lock-in amplifier. The decreased signal is compared with a set-point of the feedback circuit and the resulting difference is fed back to the scanner via the high voltage amplifier in order to control the probe-sample distance during scanning. During the scan, the phase and amplitude of the quartz tuning fork oscillations are also recorded.

5. Tuning the quality factor (Q-Control)

The quality factor Q is widely used when discussing oscillators, because this property is useful for predicting the stability of the resulting frequency around the resonance [14, 23 - 26]. Furthermore, we can infer that the quality factor can be increased by injecting energy into the tuning fork during each cycle. Similarly, the quality factor can be decreased by removing energy during each cycle. These two cases can be accomplished by adding a sine wave at the resonance frequency with the appropriate phase. However, in practice, a quartz tuning fork works at a low enough frequency to allow classical operational amplifier based circuits to be used for illustrating each step of quality factor tuning.

Figure 7 illustrates a possible implementation of the circuit including an amplifier, a phase shifter, a bandpass filter, and an adder. The feedback gain defines the amount of energy fed back to the resonator during each period; the phase shift determines whether this energy is injected in phase with the resonance (quality factor increase) or in phase opposition (quality factor decrease). The resonance frequency shift was associated with a feedback loop phase that is not exactly equal to -90°. The phase shift was set manually, using a variable resistor and an oscilloscope in XY mode, until a circle was drawn by an excitation signal and by the phase-shifted signal, allowing for a small error in the setting. Figure 8 (a, b) display a measurement of the decreasing of the quality factor based on a discrete component implementation of the circuit in Fig. 7.
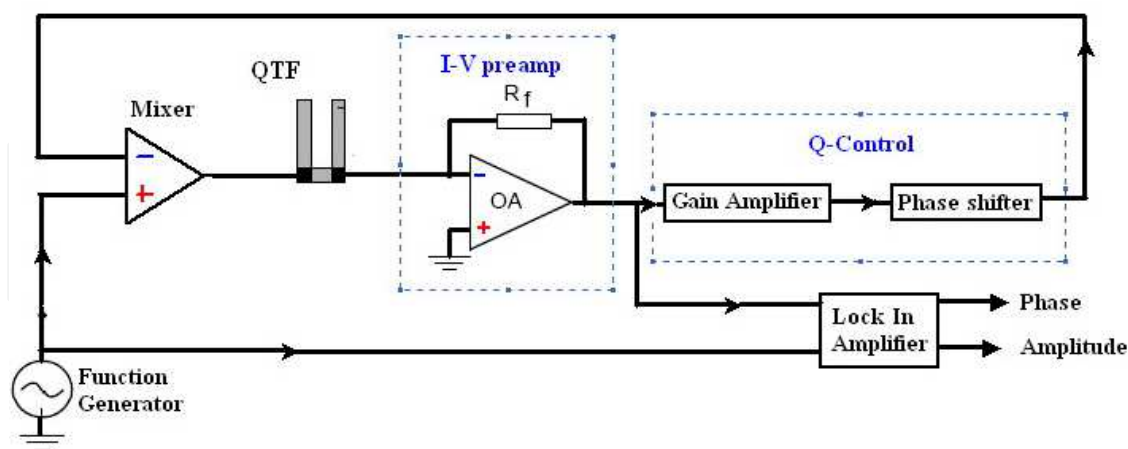

Fig. 7. Principle diagram of Q-control feedback circuit and the block diagram of I-V preamplifier and the Q-control system.

As can be seen, the tuning fork response is phase shifted and amplified before being added to the drive. The effective damping is altered by feeding back some of the response, with the phase of this feedback signal, relative to the fork velocity, determining whether the damping
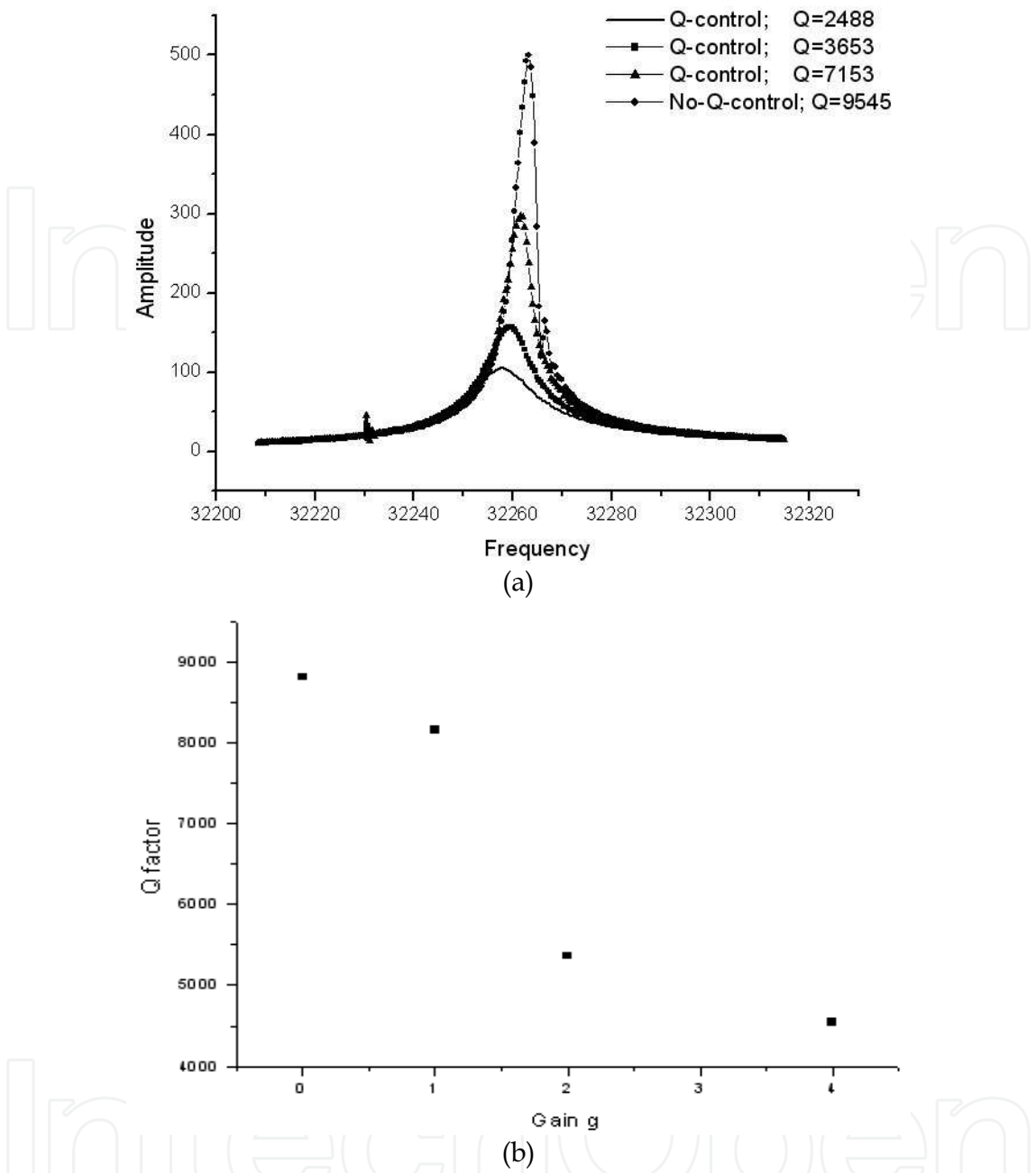
(a)

(b)

Fig. 8. Result of using Q-control, the amplitude response as a function of the driving frequency with different feedback g under condition of the phase shift -90 degree

is effectively increased or decreased. By choosing an appropriate value of the gain g, the damping of the cantilever motion is partially compensated, and hence the degree of alteration of the damping (related to Q) is changed by the gain setting.

The effect of gain g on the amplitude curves (at phase -90 degree) and constant driving force is shown in Fig. 8 (a). While the Q seems largely unchanged with the smaller gains (g<1), the increasing of g (g>1) strongly decreases the quality factor Q, oscillation amplitude, shifts the resonance frequency to lower values, and broadens the amplitude curves. This behavior is consistent with the Q-control signal adding to the damping force, not canceling it. The

Tuning Fork Scanning Probe Microscopes – Applications for the
Nano-Analysis of the Material Surface and Local Physico-Mechanical Properties

41

amplitude at resonance can be decreased by two times of magnitude with respect to the initial system, while the resonance frequency changes by a small factor (0.2%) and, as a result, g value increases from 1 to 4). Figure 8 (b) considers the effective Q as a function versus gain g, respectively. These results show that the increasing of g from 0 to 4 produces a decrease of Q of about two times of magnitude (from 8000 to 4000).

6. Fork-AFM imaging

To test the achievable resolution on our new system, a sample calibrating grating TGZ-02 was measured in two modes. The image size was about 14x14 μm² (256x256 pixels), the scan direction was from left to right, obtained with a scan rate of 0.3-0.5 Hz per line. The set point for the engaged tip vibration amplitude was fixed to about 90% of the maximum amplitude. Figures 9 (a, b) show topographical images obtained in the shear and the tapping modes, respectively. The abrupt changes in these images were attributed to instabilities such as signal drifts or tip contaminations. In the results, the effects of the radius of the tungsten tip are clearly visible. Furthermore the quality of the image shows that the tuning fork with these tip-scanners is capable of handling large variations in the height of the sample.
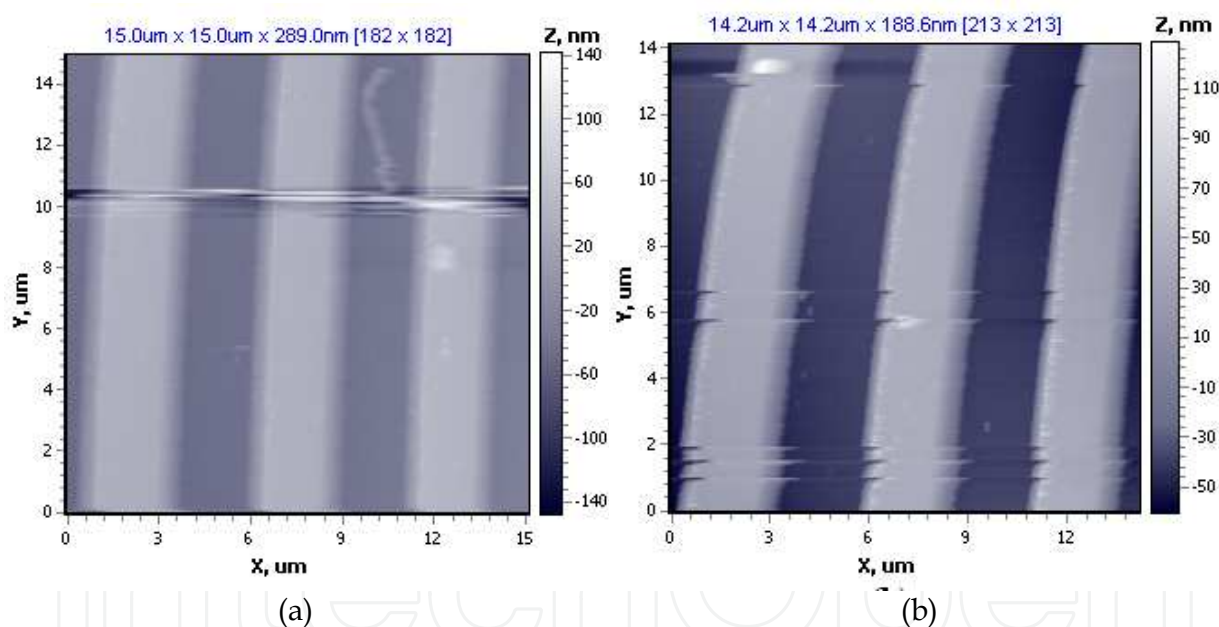

(a)   (b)

Fig. 9. Topographies obtained in (a) shear mode, and (b) tapping mode for sample calibration grating TGZ02. The dimensions of the images are about 14x14(μmxμm).

To demonstrate that the Fork-AFMs using tungsten tips were successfully used in imaging samples in two modes: tapping and shear modes, we showed related experimental results in Fig. 10. A "rigid" sample: alumina Al2O3 and a "non-rigid" sample PVP were measured. The scanning speed of two mode operations is 0.3Hz per line, the current through the tuning fork is 3nA (the prong vibration amplitude is around 3.8nm) for shear force mode and 2nA for tapping mode. The entire image was obtained in about 15 minutes for a resolution of 256x256 pixels. The set point of the feedback circuit was set at 90% maximum amplitude on resonance.
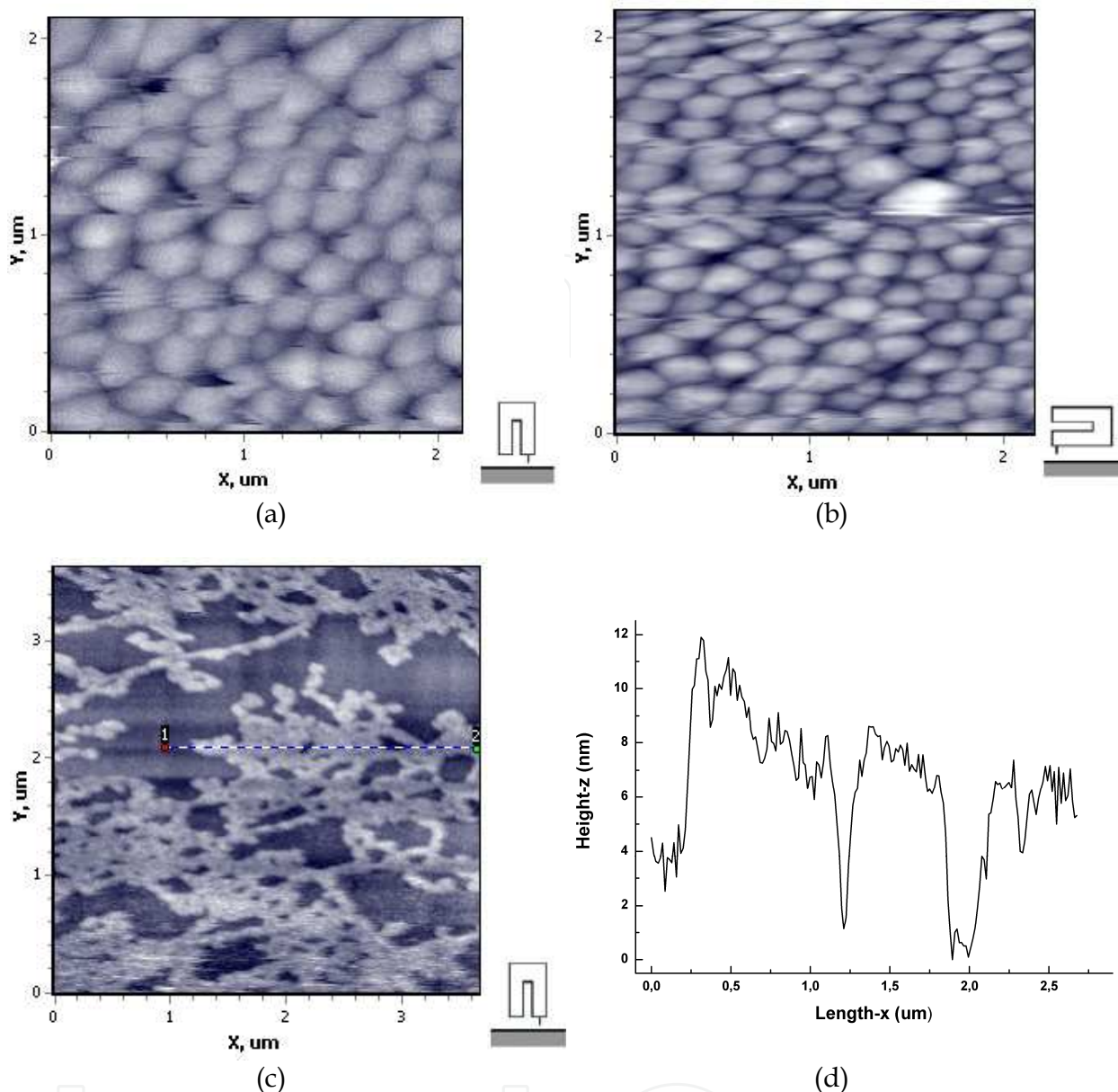
(a)

(b)

(c)

(d)

Fig. 10. Topography images of (a, b) alumina Al2O3, (c) "non-rigid" sample PVP in the shear-force and intermittent contact modes using Q-control feedback (Q<2500). The dimensions of images is noted in the figure. A line profile from 1 to 2 in (c) is show in figure (d)

By comparing images obtained in both shear mode (Fig. 10 (a)) and tapping mode (Fig. 10 (b)), we found that good images could be achieved in Fork-AFM using tungsten tips. Furthermore, a remarkable advantage of the presented technique that the length of the tungsten tips attached to the tuning fork (0.7mm) was much longer than that of commercial tips (a few micrometers). Therefore the distance between the side electrodes of the turning fork and the sample surface was much larger.

However, when using tungsten tips, the extra mass and mechanical properties of the metallic wire and the glue used to attach it to the prong can radically alter the resonance frequency (shifted by about ~ 1000Hz), and the amplitude of the oscillation and especially, the quality factor Q are significantly reduced (by more 20%). In addition to affect the

amplitude and the quality factor, the symmetry property of the oscillation of quartz tuning forks is broken because of its balance. It can affect the stability and measurement results of tuning forks with atomic force microscopes. For making balance, we usually counterbalance by a suitable mass on the other prong of a tuning fork but the amplitude and resonant frequency will suffer a rather large decrease. Moreover, the radius of tungsten tips is rather large, about 30-70nm. It is not easy to consistently make small, sharp tips with reproducible properties. Thus when the oscillating average amplitude of a tip was high, especially in shear force mode, the poor contrast images were received (Fig. 10 (a), (c)).

Figures 11 (a - d) show topographical images obtained in the tapping and shear modes, respectively, of alumina Al2O3 and PVP samples in the air at room temperature when using the cantilever silicon tips. Figures 11 (a, c) show the characteristic of shear-mode images on these materials. In these images, we do not observe the long scratches caused by the vibration of tip such as tungsten tips. The appearance of the abrupt change in the shear-mode image in Fig. 11 (a, c) could be attributed to instabilities, such as signal drifts, tip or surface sample contaminations. Figures 11 (b, d) show images of the surface of the two samples in tapping mode. Similar to the case of using the tungsten tips, the resolution of images in the tapping-mode is better than the shear-force mode. This time, the topography images can be seen as clearly as in Fig. 11(a - d). Moreover, figures 11(e, f) show the averaged line profile for PVP in two modes. From this line profile, we observed the optimum signal in the tapping mode. Additionally, the average height of the features indicated in the image is about 10 nm, and the resolution is achieved to 50nm.

It is interesting to note that we could obtain the high contrast images in shear force and tapping mode operation when using the cantilever silicon tips. Using silicon tip is rather sensitive to the signal interaction because: (i) the area contact belongs to the sharp of the tips, for the cantilever tip AFMs, because the radius of tips is rather small (<10nm), when vibrating, the amplitude tip is not large, especially with the low applied control voltage, vibration is not significant, thus the region contact between tip and sample may achieve the atom interaction; (ii) due to the short tip length (10–20 μm), the distance between the side of the tuning fork body and the sample surface is very small, and consequently this distance modulation due to the oscillation of the tip may induce undesirable noise, (iii) the mass of the tip is not significant, thus it does not influence the properties of fork, especially the symmetry. As a result, we found that a much better signal control could be achieved, and we could obtain a high resolution images with the different samples with the cantilever silicon tip.

We succeeded in getting images with discernible bit line in both cases. Furthermore by comparing force images obtained in both shear mode (Fig. 11 (a, c)) and tapping mode (Fig. 11 (b, d)) with one type of tips, we found that a much better signal could be achieved in tapping mode operation. To explaining for this result, we proposed some assumptions for explanations in the following way: in the shear-force mode, because the tip oscillates parallel to the surface of sample, the area contact between tip and sample is about 30-40nm. Therefore, in this process, the instability such as signal drifts or tip contaminations may happen and influence the resulted scanning. In the intermittent contact mode, the area contact between tip and sample is much smaller than shear force mode (about 10-15nm). As a result, the region contact between tip and sample may achieve the atom interaction preventing sample damages, and we could obtain the images with high contrast resolutions. The results showed that this Fork-AFM system with a good, sharp tip can obtain high-resolution images of samples in ambient conditions.
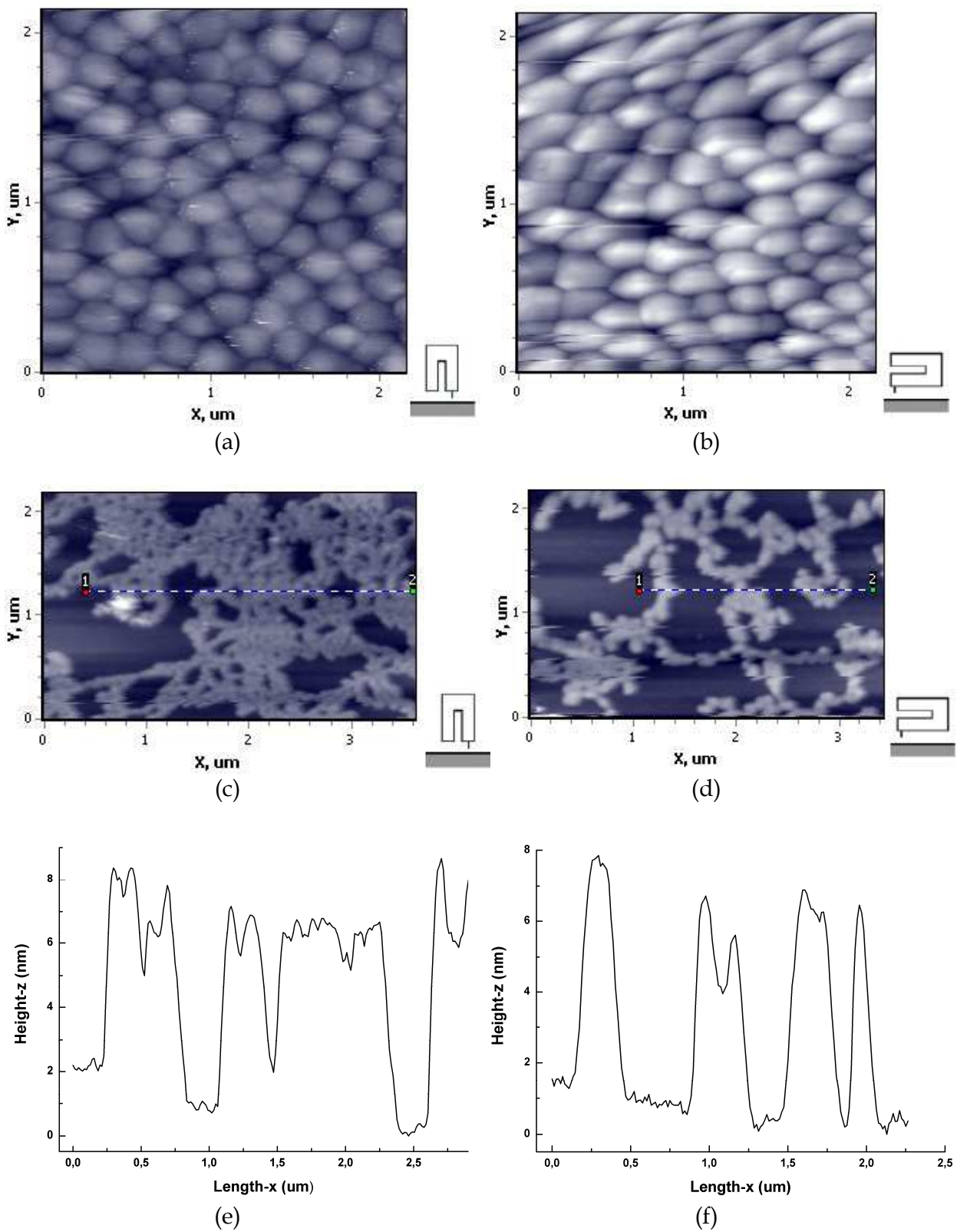
Fig. 11. Topography images of (a, b) alumina Al2O3, (c) "non-rigid" sample PVP in the shear-foce and intermittent contact mode using Q-control feedback (Q>9500). The dimension of images is noted in the figure. A line profile from 1 to 2 in (c, d) is show in figure (e, f)

We also developed a Fork-AFM system for investigations of human blood cell morphology, namely erythrocytes with high-resolution imaging. Erythrocytes samples were prepared by different ways. The first method was standard for clinical laboratory in which a drop of fresh human blood (10-20µl) was applied on a first glass surface and smeared by a second glass. The thickness of the smear decreases along a direction of smearing. In the second method, some drops of fresh human capillary blood were fixed in a 2% aqueous glutaraldehyde solution. The cover slips were rinsed with a 2% aqueous glutaraldehyde solution and washed with phosphate buffered saline (PBS). The freshly extracted blood was then diluted in PBS and this solution was then added again for 1 minute to rigidify the cell. Then the cells were washed with PBS. A preparation was dried up on air at room temperature for several hours.

Figures 12 (a - d) showed topographical images and line profile obtained in the shear force and intermittent contact modes, respectively, of erythrocytes samples in the air at room temperature. The scanning speed of two mode operations was 0.3Hz per line, the current through the tuning fork was 3nA (the prong vibration amplitude was around 3.8nm) for the shear force mode and 2nA for the intermittent contact mode. The entire image was obtained in about 15 minutes for a resolution of 256x256 pixels. The set point of the feedback circuit was set at 90% maximum amplitude on resonance.

The topography of the erythrocytes samples was obtained using shear force detection in air in Fig. 12(a). Figure 12 (b) shows the averaged line profile. From this line profile, the maximum height of the feature indicated in the image was about 1.8 µm. Furthermore, we observed the abrupt change in the shear-mode image. To explaining for the abrupt change, we bring out some assumption for explanation in the following way: in this mode, because the tip oscillates parallel to the surface of sample, the area contact between tip and sample is about 30-40nm. Furthermore, the differential height of sample is rather large. Therefore, in this process, the instability such as signal drift or tip contamination maybe appear and influence the results scanning.

Figure 12 (c) shows the topography of erythrocytes in intermittent contact mode. The image in Fig. 12 (c) can be seen as more obviously than the result in Fig. 12 (a). From this line profile (Fig. 12 (d)), the maximum height in the image is about 2.3 µm. Clearly, in this mode, the area contact between tip and sample is much smaller than shear force mode (about 10nm). As a result, the region contact between tip and sample may achieve the atom interaction, thus it prevents sample damage, and we could obtain the images with high contrast resolution.

7. Fork-AFM in analysis of property surface [29]

In this section we describe the measurement of the tip-sample interactions of a tuning fork with a tungsten tip in the shear-force mode operation on two classes of samples: i) samples with the "non-rigid surface" (soft) (polyethylene and fiber plastic) and ii) samples with the "rigid surface" (hard) (alumina Al_2O_3). In our study, we constructed a controllable Q-factor system, so that we could investigate the tip-sample interaction through the variation of the pre-set quality-factor (meaning the Q-factor at the free oscillation, when the tip is far from the sample surface, which we call hereafter Q_∞ for short). The results were interpreted with simple models that considered the damping forces between the tip and the surface polymer
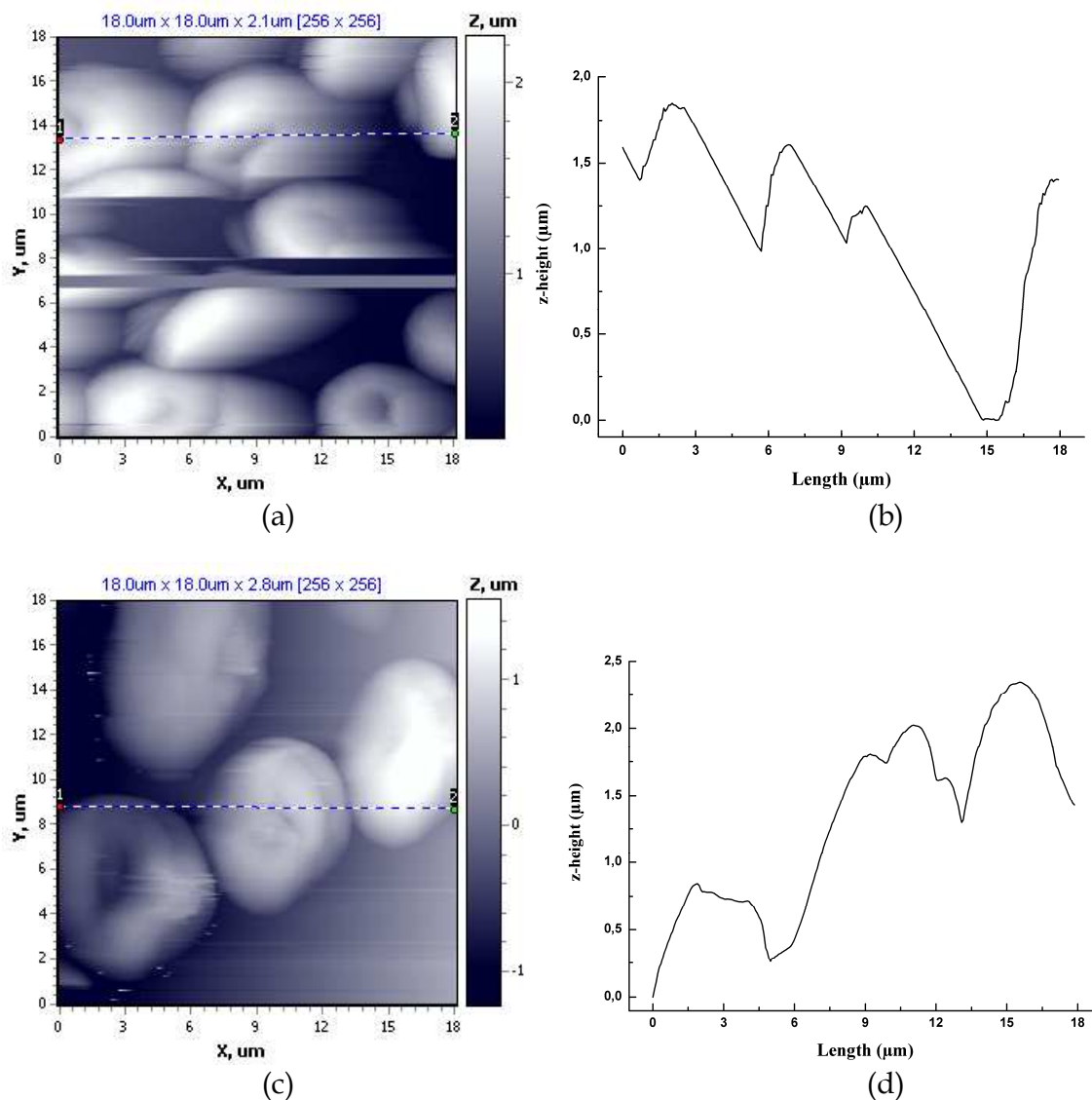
Fig. 12. (a, c) Shear force and intermittent contact mode topographical images of erythrocytes. A line profile from 1 to 2 in (a, c) is show in figure (b, d)

and the elastic forces of the polymer around the tip. The influence of the Q-factor on the interaction components of tip-sample was investigated. The results showed that the capabilities of the combination of a tuning fork and an AFM can be extended to quantitatively analyze the properties of the surface of nano-materials with high precision.

7.1 Dynamic force spectroscopy and theory of friction and elastic forces with controllable Q-factor

The amplitude-frequency-distance characteristic was measured during approach only or during retraction only to avoid backlash effects. In this measurement, we set the beginning, the final positions and the operation step of the probe. At the same time, we set up the driving frequency, ordinarily around the resonant frequency. When operating, we obtained the change of the amplitude-frequency when the tip was approaching to the surface sample very slowly. Figure 13 shows 2-D images taken in order to investigate the distance

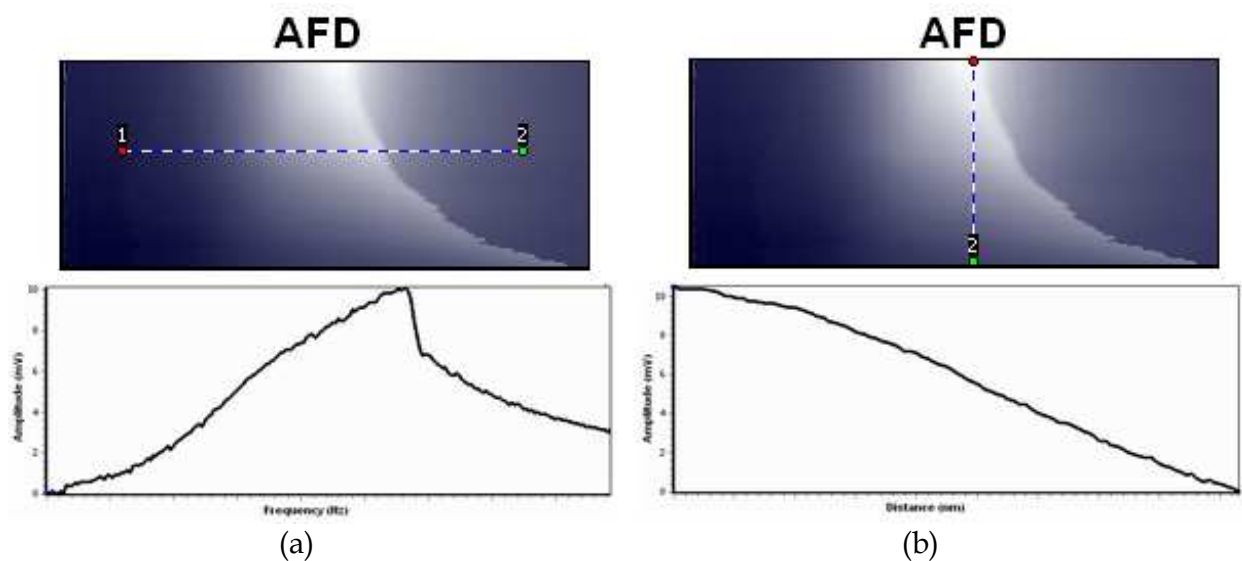(a)   (b)

Fig. 13. The 2D images of characteristic of spectroscopy amplitude-frequency-distance that operating in the dynamic shear-force. The 2-D grey scale images show the amplitude of the tuning fork vs. frequency (horizontal) and distance (vertical). In (a) the lower graph shows the amplitude as a function of frequency at fixed distance along the line 1-2 in the grey scale image; In (b) the amplitude is shown as function of distance along the line 1-2 at the resonant frequency.

dependence of these interactions on polyethylene polymer. In these images, the amplitude oscillation of the tip, that corresponded to vertical axis and defined by light-scale, was shown as a function of frequency (horizontal axis) and distance between tip and sample (vertical axis).

The tip position, d, is reported as a distance from an arbitrary reference point far from the surface, where Q-infinity is preset. An increase in d corresponds to a decrease in tip/sample separation. At each distance the amplitude is recorded as a function of frequency. All the data presented is as-measured, with no smoothing algorithms applied.

The frequency-dependent oscillation amplitude u of the arm of the tuning fork using a Q-control system obeys Newton's equation of motion given by [25, 27]:

$$\frac{\partial^2 u(t)}{\partial t^2} + \left(\gamma + \gamma_\infty + \frac{g}{\omega} \right) \frac{\partial u(t)}{\partial t} + \frac{K+k}{M} u(t) = \frac{F_D}{M} \tag{1}$$

The effective mass M of the arm, which is proportional to the mass distributed along the tine, is defined as: $M = \dfrac{K+k}{\left(2\pi f\right)^2} = 0.966 x 10^{-6} kg$. The gain g is the adjustable coefficient of Q-control system. The force F_D drives the fork harmonically at a frequency f. The damping of the motion is included in the damping rate term $\gamma + \gamma_\infty$, where gamma_inf corresponds to resonance parameters in a free oscillation. The damping rate intrinsic to the fork, where the tip disengaged from the sample, is γ. The tip-sample interaction is included in equation (1) through terms k and γ, respectively. We can then determine the tip sample-interaction-induced damping rate γ in relation to γ_∞ as

$$\gamma = \gamma_\infty \left(\frac{f_\infty u_\infty}{fu} - 1 \right) + \frac{g}{\omega}\left(\frac{u_\infty}{u} - 1 \right) \tag{2}$$

where f_∞ and f are the resonant frequency of quartz at free oscillation and at a height position, of which an interaction between tip and sample, respectively.

The damping force $F_f = M\gamma \dot{u}$ due to the tip-sample viscous damping is a drag force opposing the oscillatory motion of the tip. Using equations (1) and (2), F_f is given by:

$$F_f = \frac{i}{\sqrt{3}} \frac{Ku_\infty}{Q_\infty}\left[\left(1 - \frac{fu}{f_\infty u_\infty} \right) + \left(\frac{Q_\infty}{Q_{eff}} - 1 \right)\left(1 - \frac{u}{u_\infty} \right) \right] \tag{3}$$

Here, we introduce a new coefficient Q_{eff}, that satisfies: $\dfrac{1}{Q_{eff}} = \dfrac{1}{Q_\infty} + \dfrac{\sqrt{3}gM}{K}$.

The elastic force F_e due to the reactive tip-sample interaction, which is a restoring force along the oscillation motion of the tip, can be expressed as $F_e = ku$. The theoretical spring constant K can be obtained from $K = \dfrac{E}{4}w\left(\dfrac{t}{l} \right)^3$ where $E = 7,87 x 10^{10}\,N/m^2$ is Young's modulus of quartz. For our tuning fork - width $w \approx 0.38mm$, thickness $t \approx 0.6mm$, and length $l \approx 5.00mm$ - we obtain $K = 12\,kN/m$, which agrees reasonably well with our experimental results [22]. The local tip-sample interaction equivalent spring constant k can be obtained by using the relation for K in the equation: $k = \left[\left(\dfrac{f}{f_\infty} \right)^2 - 1 \right]K$, which gives F_e as

$$F_e = \left(\frac{f^2}{f_\infty^2} - 1 \right)Ku \tag{4}$$

To interpret expressions (3) and (4), it is necessary to define the relationship between the measured output voltage V_{out} and the oscillation amplitude of one arm of the tuning fork. The output voltage is sensitive to the asymmetric mode of the tuning fork, therefore, $V_{out} = c(u_1 - u_2)$, where c is a constant and u_1, u_2 are the amplitude of motion of the two arms of the fork. When driving the fork with an external voltage, as in our experiment, only the asymmetric mode is excited, yielding $u_1 = -u_2$. Thus, we define: $V_{out} = 2cu_1 = u_1/\alpha$, where $\alpha = 253pm/mV$ as calculated in [22].

Using equations (2), (3) and (5) and with the combination of above relationship between the measured output voltage and the oscillation amplitude of one arm of the tuning fork, we have:

$$F_f = \frac{i}{\sqrt{3}} \frac{KV_\infty}{Q_\infty}\alpha\left[\left(1 - \frac{fV_{out}}{f_\infty V_\infty} \right) + \frac{\sqrt{3}gM}{K}Q_\infty\left(1 - \frac{V_{out}}{u_\infty} \right) \right] \tag{5}$$

$$F_e = \frac{K}{f_\infty^2}\alpha\left(f^2 - f_\infty^2 \right)V_{out} \tag{6}$$

with V_∞ is the voltage corresponding to the free vibration of tuning fork. Based on these equations and the experimental data, we measured the amplitude and resonant frequency of prong of tuning fork when approaching the surface of polyethylene, and from there we determined the interaction force with surface the sample.

Figure 14(a) shows the results of the dependency between oscillation amplitude and oscillation frequency on the distance between tungsten tip and polyethylene surface where an increasing distance (d) corresponds to a decreasing tip/sample separation. We used a tuning fork with a tungsten tip having $Q_\infty = 1860$, resonant frequency 30584Hz. The applied voltage to the fork is 2.32V. As the tip approaches the surface, the amplitude *vs.* distance curve shows a monotonic decrease in amplitude. On the contrast, the resonant frequency *f* seems to increase monotonically though it is noisier. It can be seen that close to the surface of sample, the frequency reveals a more pronounced change as compared to the amplitude signal. Therefore, using modulated frequency in the near-contact region might give a better signal for distance control.
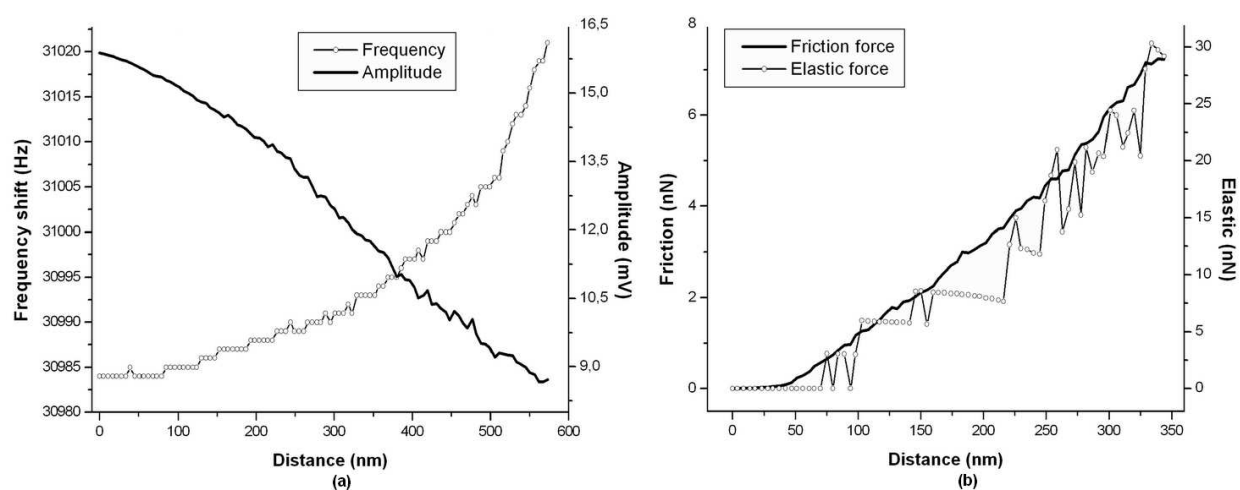
Fig. 14. The curves demonstrating the dependence of a) amplitude and frequency, b) force interactions (damping and elastic force) as a function of the tip-sample distance when the tip approaches to the surface of polyethylene. The tuning fork gluing tungsten tip with quality factor Q=1860, resonant frequency f=30584Hz, the applied voltage to the fork is 2.32V.

From the measurement results of amplitude and frequency, using equations (6) and (7) the damping and elastic forces are calculated and shown in Fig. 14 (b). The damping force changed when the separation tip-sample decreased. Similar to the damping force, the elastic interaction changed negligibly in the pre-setting contact of tip and sample. However, close to the surface, a different form of the elastic force, a "sawtooth" and "unstable" profile is observed. Therefore we could split into two interaction regions: (1) the vibrating tip is posited far from the sample; here there is no interaction between tip and sample, (2) when the tip is close to the surface of sample (the contact region), the damping force increases rapidly and monotonically. Our results of the dependence of amplitude, frequency shift, and force interactions (elastic and damping forces) in Fig. 14 (a, b) are similar to the works by Khaled Karrai et al. [27].

7.2 Influence of pre-set quality factor on parameters of tuning forks

There have been several experiments by different groups before (see, e.g., [25, 26, 28]) where the influence of a Q-control system on spectroscopy curves and on results of scanning has been investigated. But a quantitative interpretation of those experimental results is still lacking. So, for more clearly understanding, we surveyed the effect of the change of Q_∞ on the change of amplitude oscillation and quality factor of tuning fork. For a better comparison, we specifically choose one tuning fork, using the same applied voltage and measuring under the same conditions of operation, with no change of the area of the sample approached by the tip.

Firstly, we surveyed the influence of the pre-set quality-factor Q_∞ on the variation of Q factor of tuning fork during the tip approaching to the surface on these materials. Figures 15 (a, b) show the curves of quality factor versus distance for the approach on the polyethylene and alumina. We observe that the quality factor Q decreases as distance between tip-sample is reduced. For alumina the decrease of Q is rapid and rather abrupt. For polyethylene the change in Q is slow and not sudden. However, here we do not observe the influence of Q_∞ on these curves. It is seen that the variation of quality factor Q only depends on the properties of surface of materials, but not upon Q_∞. Therefore, it would be interesting to use these results for examining the general structures of the surface sample.
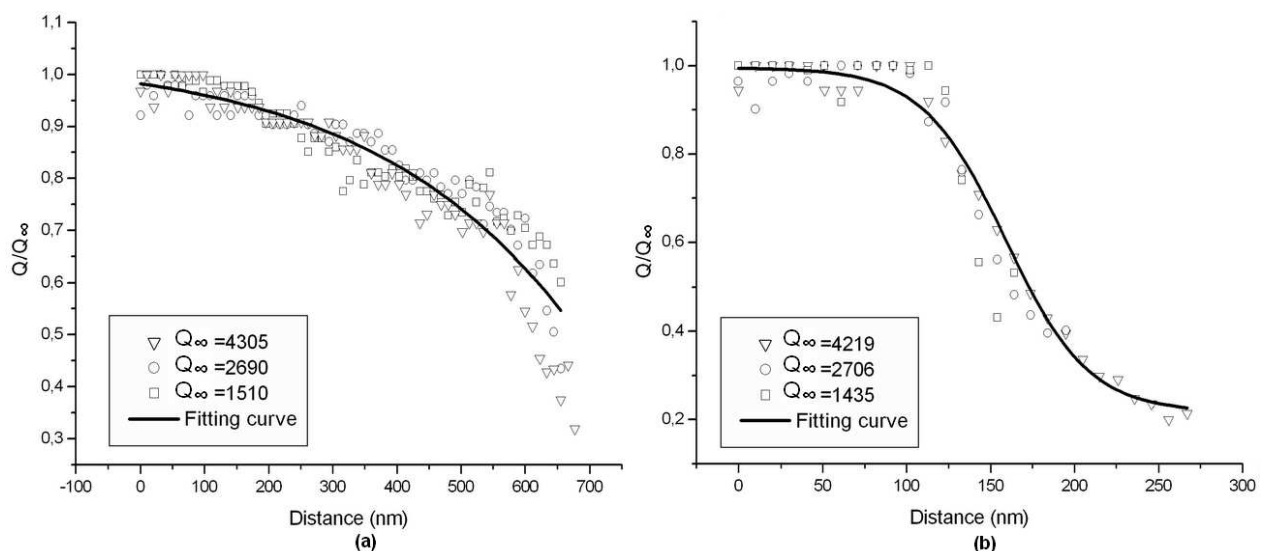

Fig. 15. The curves of the variation of quality factor versus distance between tip-sample that using the different pre-set quality factor Q_∞ on (a) fibre plastic, (b) alumina. The dark curves are the fitting curves of the experimental data.

In order to illustrate the application of the variation of quality factor Q with sample, we performed the above experiments on three materials: polyethylene, fiber plastic and alumina Al_2O_3 (in Fig. 16). We observed an obvious difference between these materials. While the change of the slope Q versus the distance between tip-sample for polyethylene and fiber is rather shallow, the result for alumina Al_2O_3 is a steep slope. Therefore we are confident that we could expand this measure to identify the surface property of the other materials: "rigid" or "non-rigid" materials.
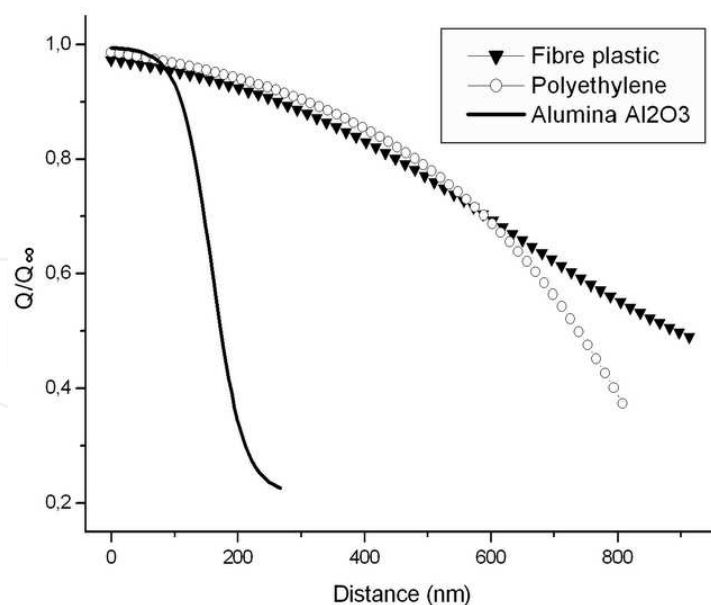
Fig. 16. The fitting of the measured data demonstrating the dependence of the change of quality factor on distance of tip-sample when the tip approaches to the surface on three samples: polyethylene, fiber plastic and alumina Al2O3.

In order to understand the observed material dependence of the variation of Q during the tip approaching the surface, we make some assumptions for two classes of materials: for the alumina sample, the property of surface is rather homogeneous, and has a rigid structure. In the shear-force mode, the tip oscillates horizontally. On the tip abruptly enters the influence region of the atomic forces. Therefore the variation of the interaction curves of alumina sample is rather abrupt. In contrast, the surface of polyethylene or fiber plastic has no tight structure and is not smooth. The influence of the atomic forces is not uniform and there is not a clear bound of the interaction region. So when approaching closer to the "non-rigid" sample, the tip is not affected suddenly, but rather smoothly. This observation may be very useful for surveying the properties of surface for the different types of samples.

As mentioned above, the variation of the quality factor Q during the tip approach is not affected by the change of Q_∞. On the other hand, the change of the amplitude oscillation is strongly affected by the change of Q_∞. To understand this effect, we measured the change of the amplitude oscillation of the tip as it approached closer to the sample using different pre-set Q_∞ on three samples: polyethylene, fiber plastic, alumina, as shown in Fig. 17 (a - c). For alumina, the larger Q_∞ resulted in the shallower slope of the curve of the change amplitude versus distance between tip-sample. However the trends differed for polyethylene and fibre plastic. Furthermore, we realized that for "non-rigid" materials, at positions closer to the sample, the amplitude oscillation of the tip increased when Q_∞ decreased. We did not observe this behavior on alumina. These results explained that we could be able to obtain the information about images as well as the properties of the surface of "non-rigid" samples more advantageously when reduced Q_∞. It is suitable for the observations that we could achieve the best scan rate and obtained the real time imaging and high resolution with low quality factor Q_∞ [25].
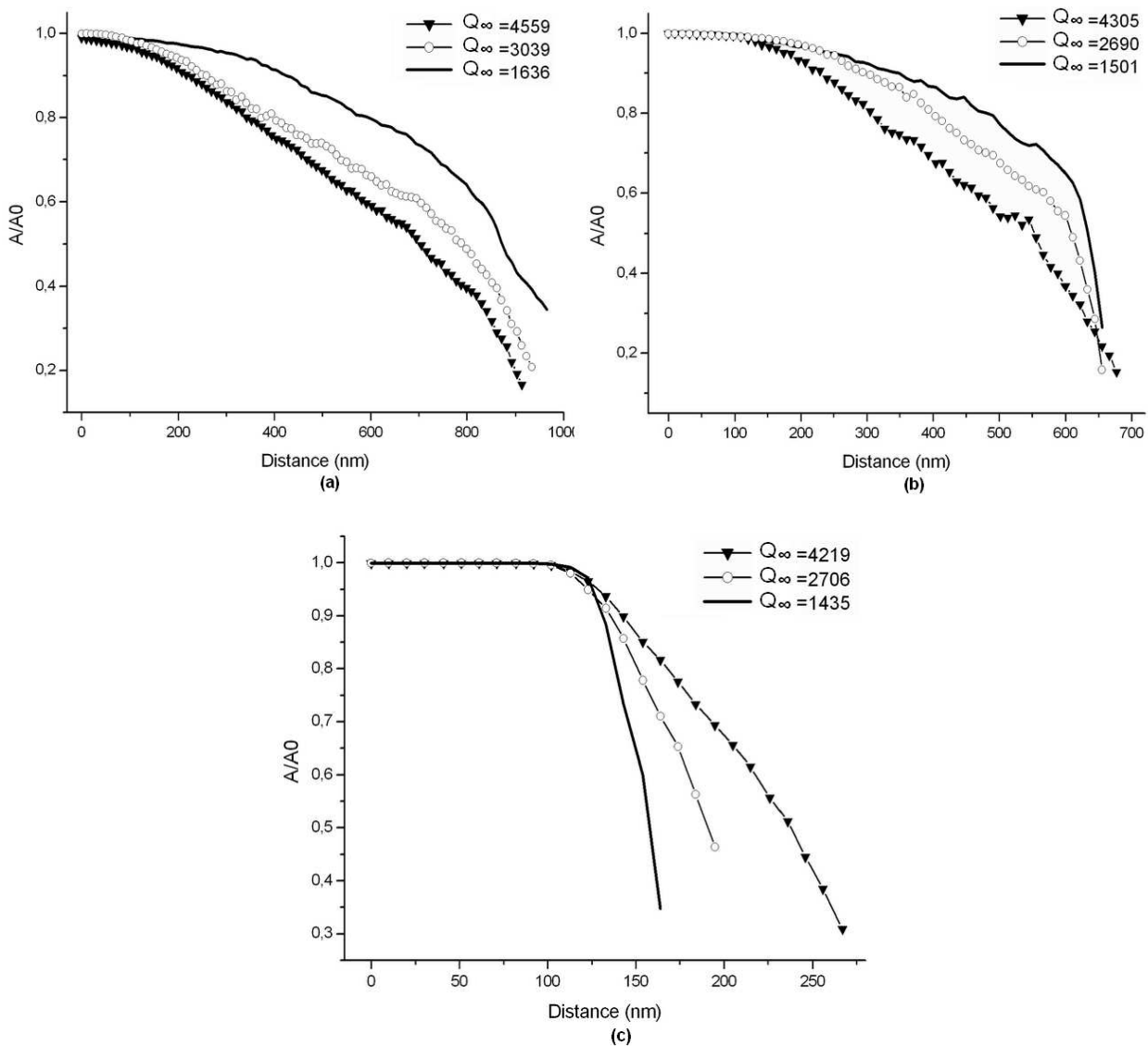
Fig. 17. The amplitude dependence on tip-sample distance for three pre-set quality factor Q_∞ on (a) polyethylene, (b) fiber plastic, (c) alumina Al2O3.

7.3 Influence of pre-set quality factor on the force interactions

Figures 18 (a - d) showed the resulting force interaction curves with the different pre-set quality factors on the "soft" material: polyethylene, and "rigid" material: alumina (Al_2O_3). A clear effect of the variation of factor Q_∞ on the damping force is observed for "soft" materials (polyethylene or fiber plastic). At the same distances between the tip and sample, corresponding to lower preset factors Q_∞, the damping force is larger (Fig. 18 (a)). These results demonstrated that further reduction of damping force can be achieved by decreasing the fork's quality factor. We predicted that with the "soft" materials in the semi-contact and contact regimes we could change the quality factor and therefore increased the effective tip-sample interaction, leading to higher stabilization in shear-force operation. In contrast, for alumina, the major difference was observed in the results of the curves of the damping force. In Fig. 18 (c), the damping force for alumina depended on the change of the pre-set Q_∞.
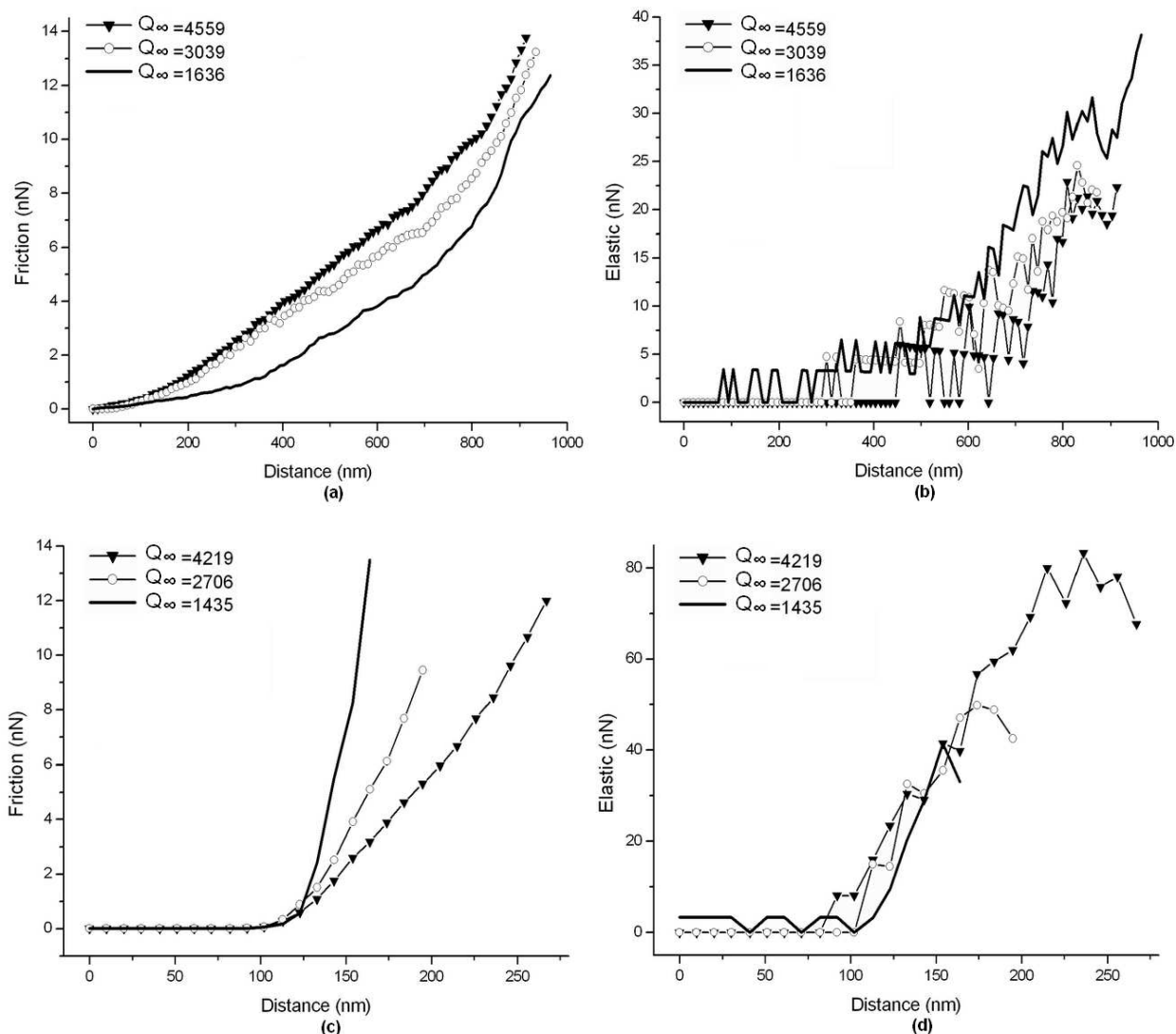
Fig. 18. The force spectroscopy curves demonstrating the influence of the change of the free quality factor on force interactions (damping and elastic force) when the tip approaches to the surface of (a, b) polyethylene sample; (c, d) alumina Al2O3.

However, the larger Q_∞, the smaller the variation of the slope curves of the damping force. We do not compare the increase of the damping force at the positions closer to samples corresponding to the three different pre-set quality factors Q_∞.

8. Discussions and conclusions

We have discussed the quartz tuning fork, a two-terminal electronic component whose use is essential in applications that require an accurate time reference. We have also demonstrated atomic force microscopies using quartz tuning with and without Q-control fork in air conditions in two operation modes: shear force and intermittent contact modes. The scanning time can be reduced so that for the images of smaller size one can acquire high resolution images almost in real time, which may allow the recording of high resolution videos. Reproducible topographic images have been obtained on hard and soft samples. Furthermore, it suggested that Fork-AFMs can become a very useful and reliable tool in the

study of biomolecules. The obtained results showed that the capabilities of the combination of AFM and tuning fork could enable quantitatively analyses of the properties of surface with high precision and resolution.

Furthermore, we have measured the dynamic spectroscopy of amplitude-frequency-distance and developed a model to determine the force interactions (damping and elastic forces) using tuning fork gluing tungsten tips in shear-force mode. A survey of the influences of the pre-set quality factor (by using the Q-control) on the interaction components between the tip and sample was presented. They also opened up new ways to explain the advantages of using the low pre-set quality factor for tuning forks to get better information on the surface of "non-rigid" materials. In the future, this will provide a framework to extend applications of the tuning fork based on AFM in qualitative analysis in nanotribology, and to provide insight into determinations of parameters and properties of surface of soft material, such as selection of structure surface of materials, viscosity coefficient and shear modulus.

9. Acknowledgments

10. References

[1] Binnig, G.; Quate, C. F. & Gerber, C. (1986). Atomic force microscope, *Phys. Rev. Lett.*, Vol. 56, pp. 930-933

[2] Tran Xuan Hoai; Tran H. Hung; Au D. Tuan; Phan Canh; Phung T. Thuc & Vo T. Tung (2004). Design a DSP controlling atomic force microscope working with Linux operating system, *Proceeding of ICT.rda'04, Hanoi*, pp. 31-39, Vietnam, September 18-20, 2004

[3] Guethner, P.; Fischer, U. & Dransfeld, K. (1989). Scanning near-field acoustic microscopy, *Appl. Phys. B. Photophys. Laser Chem.*, Vol. B 48, pp. 89-92

[4] Giessibl, F.J. (1998). High-speed force sensor for force microscopy and profilometry utilizing a quartz tuning fork, *Appl. Phys. Lett.*, Vol. 73, pp. 3956-3958

[5] Karrai, K. & Grober, R.D. (1995). Piezoelectric tip-sample distance control for near field optical microscopes, *Appl. Phys.Lett.*, Vol 66, pp. 1842-1844

[6] Giessibl, F.J. (1989). High-speed force sensor for force microscopy and profilometry utilizing a quartz tuning fork, *Appl. Phys. Lett.*, Vol. 73, pp. 3956-3958

[7] Rychen, J.; Ihn, T.; Studerus, P.; Herrmann, A. & Ensslin, K. (1999). A low-temperature dynamic mode scanning force microscope operating in high magnetic fields, *Rev. Sci. Instrum.*, Vol. 70, pp. 2765-2768

[8] Zang, J. and O'Shea,S. (2003). Tuning forks as micromechanical mass sensitive sensors for bio- or liquid detection, *Sensor and Actuator*, Vol. 94, pp. 65-72

[9] Rensen, W. H. J. (1995). Imaging soft samples in liquid with tuning fork based shear force microscopy, *Appl. Phys.Lett.*, Vol. 66, pp. 1842-1844

[10] Karrai, K. and Tiemann, I. (2000). Interfacial shear force microscopy, *Phys. Rev. B*, Vol. 62, pp. 13174-13181

[11] Tamayo, J.; Humphris, A.D.L. & Miles, M.J. (2000). Piconewton Regime Dynamic Force Microscopy in Liquid, *Appl. Phys. Lett.*, Vol. 77, pp. 582

[12] Antognozzi, M.; Binger, D.R.; Humphris, A.D.L.; James, P.J. & Miles, M.J. (2001). Modeling of cylindrically tapered cantilevers for transverse dynamic force microscopy (tdfm), *Ultramicroscopy*, Vol. 86, pp. 223

[13] Bhushan, B. (2006). *Springer Handbook of Nanotechnology* 2nd, Springer, Heidelberg

[14] Lei, F.H.; Nicolas, J.-L. & Troyon, M. (2003). Shear force detection by using bimorph cantilever with the enhanced Q-factor, *J. Appl. Phys.*, Vol. 93, pp. 2236–2243

[15] M. P. Forrer, (1969). A flexure-mode quartz for an electronic wrist-watch, *Proceedings 23rd ASFC Ann. Symp. on Frequency Control*, pp. 157–162

[16] Yoda, H.; Ikeda, H. & Yamabe, Y. (1972). Low power crystal oscillator for electronic wrist watch, *Proceedings 26th ASFC Ann. Symp. on Frequency Control*, pp. 140–147,

[17] Ong, P. P. (2002). Little known facts about the common tuning fork, *Phys. Educ.*, Vol. 37, pp. 540–542

[18] Matsiev, L.F. (1999). Application of flexural mechanical resonators to simultaneous measurements of liquid density and viscosity, Ultrasonic symposium, Vol. 1, pp. 457–460

[19] Chuang, S.S. (1981). Quartz Tuning Fork Crystal Using Overtone Flexure Modes, 35th Annual frequency control symposium, pp. 130–143

[20] Itoh, H.; Aoshima, Y. & Egawa, T. (2001). Model of a quartz crystal tuning fork using torsion spring at the joint of the arm and the base, *Proceedings* of the 2001 IEEE International Issue Date, pp. 592–596

[21] Blaauwgeers, R.; Blazkova, M.& Človečko, M. (2007). Quartz tuning fork: thermometer, pressure – and viscometer for Helium liquids, *Low temperature physics*, Vol. 146, pp. 537–562

[22] Vo Thanh Tung, Chizhik, S.A.; Chikunov, V.V.; T.V. Nguyen & X.H. Tran (2006). Influence of additional mass on quartz tuning fork in dynamic operation mode, *Proceeding of 7th Int. BelSPM-7*, Belarus, pp. 236–240

[23] Lei, F.H.; Angiboust, J.F.; Qiao, W. (2004). Shear force near-field optical microscope based on Q-controlled bimorph sensor for biological imaging in liquid, *Journal of Microscopy*, Vol. 216, pp. 229–233,

[24] Vo Thanh Tung (2008). Influence of Q-control on Shear-force Detection with Quartz Tuning Fork in Atomic Force Microscopy, *Молодежь в науке – 2007: прил. к журн. «Весці Нацыянальнай акадэміі навук Беларусі». – Минск: Белорус. наука*, Vol. 3, pp. 85–89

[25] Vo Thanh Tung & Chizhik, S.A. (2007). Quartz tuning fork atomic force microscopy using quality-factor control, *Proceeding. of Int. Physics, Chemistry and Application of Nanostructures: Reviews and Short Notes to Nanomeeting-2007 Minsk, Belarus, (World Scientific Pub Co Inc.)*, pp. 535–538

[26] Friedt, J.-M. & Carry, É. (2007). Introduction to the quartz tuning fork, *Am. J. Phys.*, Vol. 75, pp. 415–422,

[27] Karrai, K. & Tiemann, I. (2000). Interfacial shear force microscopy, *Phys. Rev. B*, Vol. 62, pp.13174-13181

[28] Callaghan, F. D.; Yu, X. & Mellow, C. J. (2005). Variable temperature magnetic force microscopy with piezoelectric quartz tuning forks as probes optimized using Q-control, *App. Phys. Lett.*, Vol. 87, pp. 214106

[29] Vo Thanh Tung; Chizhik,S. A. & Tran Xuan Hoai (2009). Parameters of tip–sample interactions in shear mode using a quartz tuning fork AFM with controllable Q-factor, Journal of Engineering Physics and Thermophysics, Vol. 82, No. 1, pp. 140-148
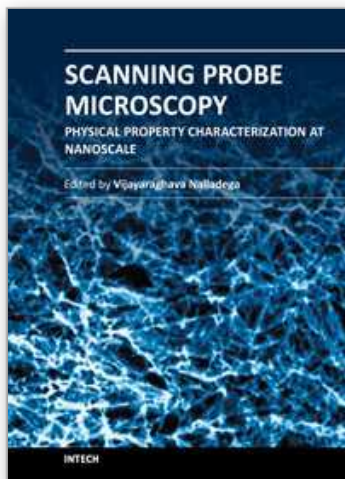
Scanning probe microscopy (SPM) is one of the key enabling tools for the advancement for nanotechnology with applications in many interdisciplinary research areas. This book presents selected original research works on the application of scanning probe microscopy techniques for the characterization of physical properties of different materials at the nanoscale. The topics in the book range from surface morphology analysis of thin film structures, oxide thin layers and superconducting structures, novel scanning probe microscopy techniques for characterization of mechanical and electrical properties, evaluation of mechanical and tribological properties of hybrid coatings and thin films. The variety of topics chosen for the book underlines the strong interdisciplinary nature of the research work in the field of scanning probe microscopy.

INTECH
open science | open minds